

6C.3 OCEANIC HEAT CONTENT VARIABILITY IN EASTERN PACIFIC OCEAN

Jodi K. Brewster and Lynn K. Shay
Division of Meteorology and Physical Oceanography
Rosenstiel School of Marine and Atmospheric Science
University of Miami

1. INTRODUCTION

Coupled oceanic and atmospheric models to accurately predict hurricane intensity and structure change will eventually be used to issue forecasts to the public who increasingly rely on the most advanced weather forecasting systems to prepare for landfall (Marks et al. 1998). The Eastern Pacific Ocean basin (EPAC) is a region of significant upper oceanic variability given the warm pool and shoaling of the thermocline, and westward propagation of warm-core rings (WCR). As easterly waves move over the EPAC, tropical cyclogenesis often begins over the warm pool. This regime is characterized by large sea surface temperature (SST) gradients and oceanic heat content (OHC) variations that impact hurricane intensity. Thermal gradients across the ocean mixed layer base (OML) are sharp starting about 40 m beneath the surface and the 20°C isotherm separates the upper from the lower layer in a two-layer model. Given the strength of buoyancy frequencies (N) of ~20 cph, wind-driven current shear tends to be insufficient to significantly cool the upper ocean through shear instability until hurricanes move west-northwest where N is weaker. Hence, a larger fraction of the OHC is available to storms via air-sea fluxes.

To understand this EPAC upper ocean variability, the Eastern Pacific Investigation of Climate (EPIC) field program, was conducted in and over the warm pool and along the 95°W to improve our understanding of these upper ocean processes and determine their relationship to the atmosphere boundary layer (Figure 1). During the field program (Raymond *et al.*, 2004), oceanic current, temperature and salinity measurements from Airborne eXpendable Current Profilers (AXCP), Airborne eXpendable Conductivity Temperature and Depth (AXCTD) profilers and Airborne eXpendable Bathythermographs (AXBt) were acquired from NOAA WP-3D and NCAR WC-130 research aircraft. Profilers were deployed from 19 research flights encompassing the warm pool/ITCZ and along the 95°W

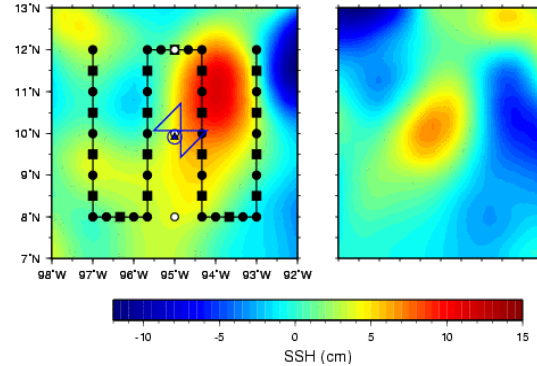


Figure 1: Sept (left) and Oct (right) SSH Anomaly (cm) fields based on a blended 0.33° gridded analysis of radar altimetry relative to aircraft sampling pattern where AXCP (boxes) and AXCTD (circles) relative to the *R/V Brown* sampling at 10°N, 95°W TAO mooring and Sea-Soar sections by the *R/V New Horizon*.

equatorial transects in Sept and Oct 01 (Fig. 1). Oceanic profilers were complemented with flight-level winds and atmospheric profiler data from GPS sondes. Flight tracks were located on each side of the *R/V Brown* and *R/V New Horizon* centered on the 10°N TAO mooring (Wijesekera *et al.* 2005).

The sea surface height (SSH) anomaly field reflects a WCR with a diameter about 120 km as it propagated west to southwest at $\sim 14 \text{ cm s}^{-1}$, consistent with a Rossby wave. Hansen and Maul (1991) hypothesized that these rings are formed when North Equatorial Counter Current (NECC) approaches the eastern boundary during times of the maximum strength in boreal autumn. A second hypothesis is that low-level atmospheric jets form WCRs over the Gulfs of Panama and Tehuantepec. In section 2, vertical structure measurements are described. In section 3, the observed WCR is tracked from *in situ* data. In section 4, satellite data are used to determine the phase speed and pathway of the warm eddy and the implications for hurricane Juliette followed by a summary in section 5.

2. VERTICAL STRUCTURE

Beginning 12 Sep, the *R/V Brown* was on station at 10°N, 95°W acquiring measurements until 1 Oct. Mean

Corresponding Author Address: Lynn K. Shay, MPO, RSMAS, 4600 Rickenbacker Causeway, Miami, FL 33149. Email: nshay@rsmas.miami.edu.

temperature, salinity, and density profiles from the *Brown* CTD are compared to XCTDs on 13, 16 and 20 Sept. Mean temperature from XCTD profiles indicate an OML temperature of 28.8°C. Temperature gradients were similar to 70 m where XCTDs suggest slightly warmer water than the *Brown* CTD. Observed profiles converged at ~200 m and have similar structure to 500 m. Salinity profiles indicated consistent results despite the separation of O(100 km). As shown in Figure 2, the scatter of the mean profiles suggests that the AXCTDs performed within vendor specifications.

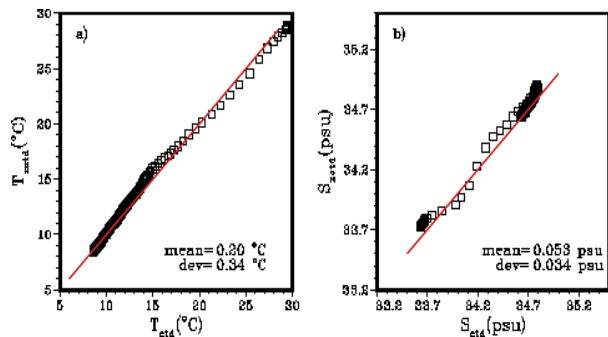


Figure 2: Scatter of mean *R/V Brown* and surrounding AXCTD a) temperatures (°C) and b) salinities (psu) relative to the perfect fit (solid red line) at 10°N, 95°W.

Meridional sections in the grid indicate T-S variability from Sep and Oct (Figure 3). T-S diagrams indicate more variability along 93°W and 94.3°W than along the other sections, consistent with the *Brown* observations of a marked water mass change on 21 Sep. This is also consistent with the observed eddy moving southwestward. Compared to climatologies (Teague *et al.* 1990), *in situ* data exhibit more variability in the upper 100 m, and that the observed N are 3 to 6 cph higher (not shown), which has implications for the OML budgets (Jacob and Shay 2003).

3. ISOTHERM DEPTHS AND OHC

As the ITCZ migrates northward during the boreal summer, there is a seasonal surface wind dependence, that aids in the formation of an upwelled Costa Rican Dome (Hofmann *et al.* 1981). The CRD regime ranges from 200 to 400 km with its' center located between 8 to 10°N at about 90°W, just east of the 93°W transect (see Fig. 1). Early studies suggested that the CRD is a permanent feature due to the cyclonic rotation of the circulation associated with North Equatorial Current (NEC) and NECC (~6°N). Hofmann *et al.* (1981) found

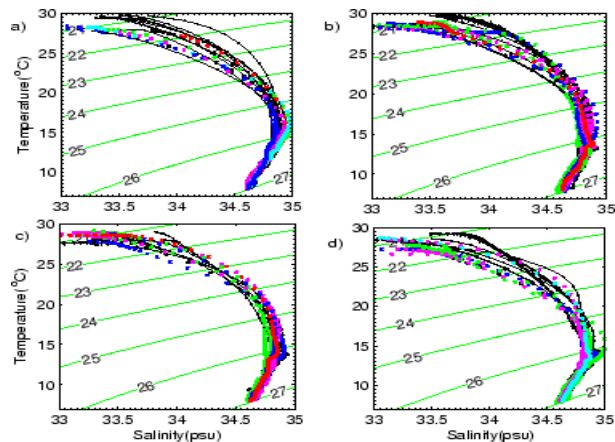


Figure 3: Meridional XCTD sections along a) 93°W, b) 94.3°W, c) 95.6°W and d) 97°W for Sept (black) and Oct (color) measurements.

that the upwelled dome exists only seasonally due to positive stress curl over the EPAC. The 20°C isotherm depths (Figure 4) on each side of the warm ring, based on seven snapshots, range from over 45 m to less than 20 m suggestive of the CRD. This dome forces a balanced circulation that affects the warm pool circulation (Kessler 2002). OHC values estimated from these snapshots (Figure 5) typically range between 50-55 kJ cm⁻² compared to more than 100 kJ cm⁻² in the Loop Current. Time series from a TAO mooring reveals similar levels (Figure 6).

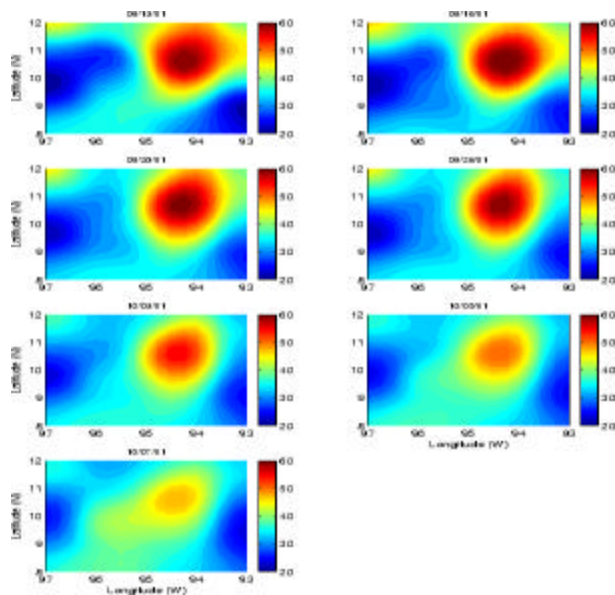


Figure 4: 20°C isotherm depth (m: color) from the seven snapshots based on the aircraft sampling.

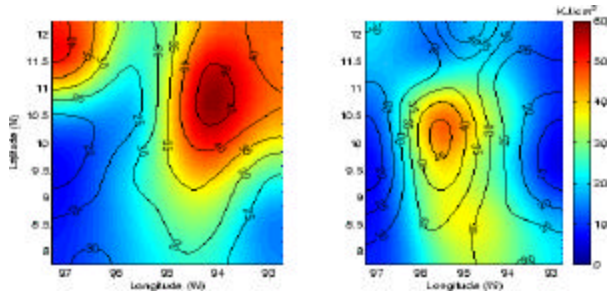


Figure 5: OHC (kJ cm^{-2}) from Sept (left panel) and Oct (right panel) based on profiler data.

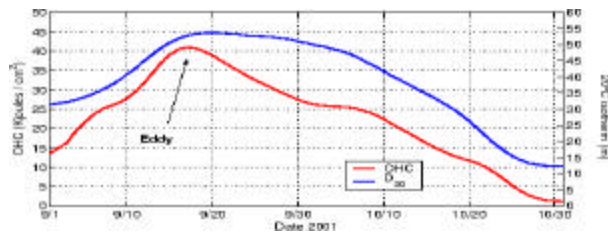


Figure 6: Time series of OHC (red) relative to 26°C isotherm depth and the 20°C isotherm depth (blue) at $10^{\circ}\text{N}, 95^{\circ}\text{W}$ TAO mooring (Cronin et al. 2002).

Non-local atmospheric events impact the mesoscale warm pool variability and the generation of warm and cold eddies along the coastline. Wind events are associated with low-level atmospheric jets occurring downstream from the mountain gaps. These Tehuantepec and Papagayo Jets persist for time scales of a few days when cold air outbreaks occur on one side of the coastal mountain range that set up a large-scale pressure gradient causing air to pour through the gaps (Hurd 1929). Gap wind jet signatures are evident in annual mean winds despite their transient nature during the boreal winter with a secondary peak during the summer (Kessler 2002). A second possibility for warm eddy generation is through shear-instabilities of the NEC and NECC (Hansen and Maul 1991).

4. SATELITE TRACKING

NASA's TOPEX/ Poseidon (T/P) and Jason-1 altimeter measures the sea level every 9.9 days along repeat ground-track spaced 3° longitudinally at the Equator. ERS-2 mission and NOAA Geosat Follow-On-Missions (GFO) have repeat tracks of 35 and 17 days, respectively. The availability of SSH data from altimeter missions allow us to extend the analysis back in time to estimate parameters involved here (see: http://www.jason.oceanobs.com/html/donees/produits/satellites_uk.html for a merged satellite product available 1992-2005 from AVISO).

Weekly SSHs are used to track eddies from Aug through Oct 2001 using the AVISO product (Figure 7). By the time the eddy reaches the center of the EPIC domain, it starts to spin down as suggested by Figure 4. The ring pathway is tracked over a three-month period based successive images. The translation speed is $\sim 13 \text{ cm s}^{-1}$ towards the west southwest, in accord with White (1977). The WCR diameter ranges from 60 to 120 km based on this 6 cm SSH anomaly. Using several years of AVISO images may help us understand how these warm ocean features project unto seasonal and intra-seasonal scales as they are key component to the ocean circulation (Hansen and Maul 1991).

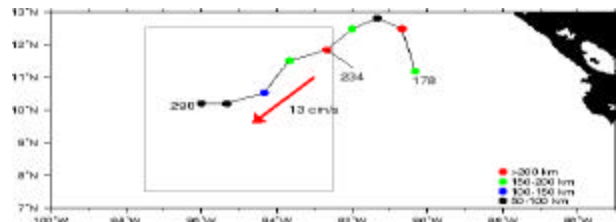


Figure 7: Pathway and size (color) of an observed WCR during EPIC experiment (box) from a sequence of AVISO SSH images starting in 25 June (Yearday 178) and ending in 17 Oct 01 (YD 290). The eddy scale, based on the radius to a 6-cm SSH, shows a spin-down of the eddy in the EPIC domain.

Warm rings have important geophysical consequences in and above the warm pool by interacting with the CRD circulation and providing heat to the atmosphere during cyclogenesis. Raymond et al. (2004) documented several tropical systems that developed during EPIC most notably Juliette (20 Sep). As shown in Figure 8, she rapidly intensified from a tropical storm to a category 4-storm northeast of the warm pool in less than a day. SST cooling from the TRMM Microwave Imager, ranged from about 1°C just north of the warm pool to 6°C in a region of weak stratification.

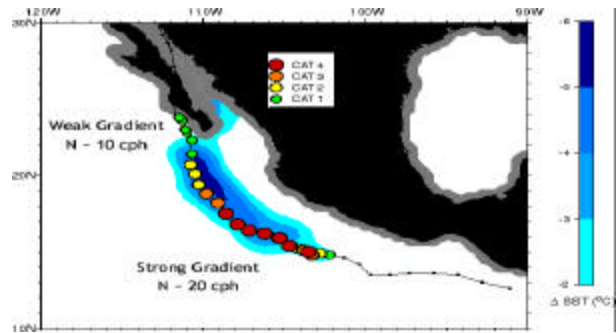


Figure 8: SST changes ($^{\circ}\text{C}$: color) induced by hurricane Juliette (Sept 01) relative to strong and weak N.

5. SUMMARY

The eastern Pacific Ocean basin responds to both short-term weather events such as hurricanes (Raymond *et al.* 2004) and gap winds (Kessler 2002), as well as forming the Costa Rica Dome (Hofmann *et al.* 1981) through the mean wind stress and curl. The EPIC data acquired during EPIC in addition to the TAO moorings (Cronin *et al.* 2002) and satellite altimetry must be used to improve our understanding of the effects of transient and mean wind conditions on the upper ocean and assess the impact of warm rings on atmospheric processes. Implicit in satellite algorithms is the acquisition ocean structure measurements including the moored TAO array data (Cronin *et al.* 2002).

The integrated thermal structure (OHC) is a more effective measure of the ocean's influence on storm intensity than just SST. In this context, upper ocean structure must be accurately accounted for in the models with realistic ocean mixing parameterization schemes based on measurements. While thin OML deepen and cool quickly through shear instability (Price 1981; Shay 2001; Jacob *et al.* 2000) and induce negative feedback to the atmosphere, the strong stratification at the base of the OML and the long inertial periods of 2 to 3 days may preclude significant cooling during genesis and passage over the EPAC warm pool. Thus, more heat is available to the storm or reduced negative feedback as the upper ocean does not significantly cool that quickly.

Acknowledgments: The National Science Foundation OCE-00-02459 and ATM-00-02363, and NOAA JHT NA17RJ1226 have supported Research effort. We are grateful for the efforts of the pilots, technicians, engineers and scientists at NOAA's Aircraft Operation Center (Dr. Jim McFadden, Captain Sean White). Tom Cook provided the graphics. John Lyman provided the processed AVISO images.

6. REFERENCES

Cronin, M. F., N. Bond, C. Fairall, J. Hare, M. J. McPhaden, and R. Weller, 2002: Enhanced oceanic and atmospheric monitoring underway in the Eastern Pacific. *EOS*, **83(19)**, 210-211.

Hansen, D. V., and G. A. Maul, 1991: Anticyclonic current rings in the eastern tropical Pacific Ocean. *J. Geophys. Res.*, **96**, 6965-6979.

Hofmann, E., A. Busalacchi, and J. J. O'Brien, 1981: Wind generation of Costa Rica Dome, *Science*, **214**, 552-554

Hurd, W.E., 1929. Northers of the Gulf of Tehuantepec. *Mon. Wea. Rev.*, **57**, 192-194.

Leipper, D., and D. Volgenau, 1972: Hurricane heat potential of the Gulf of Mexico. *J. Phys. Oceanogr.*, **2**, 218-224.

Jacob, D. S., and L. K. Shay, 2003: The role of oceanic mesoscale features on the tropical cyclone-induced mixed layer response: a case study. *J. Phys. Oceanogr.*, **33**, 649-676.

Kessler, W.S. 2002: Mean Three-Dimensional circulation in the Northeast Tropical Pacific. *J. Phys. Oceanogr.*, **32**, 2457-2471.

Price, J. F., Upper ocean response to a hurricane. *J. Phys. Oceanogr.*, **11**, 153-175.

Raymond, D. J., S. K. Esbensen, C. Paulson, M. Gregg, C. Bretherton, W. A. Peterson, R. Cifelli, L. Shay, C. Ohlmann, and P. Zuidema, 2004: EPIC2001 and the coupled ocean-atmosphere system of the tropical East Pacific. *Bull. Amer. Met. Soc.*, 85(9), 1341-1354.

Shay, L. K., 2001: Upper Ocean Structure: Response to Strong Forcing Events. *In: Encyclopedia of Ocean Sciences*, ed. R.A. Weller, S.A. Thorpe, J. Steele, Academic Press International, London, UK, 3100 - 3114

Shay, L. K., G. J. Goni, and P. G. Black, 2000: Effect of a warm oceanic feature on hurricane Opal. *Mon. Wea. Rev.*, **128**, 1366-1383.

Teague, W.J., M.J. Carron, and P.J. Hogan, 1990: A comparison between the Generalized Digital Environmental Model and Levitus climatologies. *J. Geophys. Res.*, **95**, 7167-7183.

Wijesekera, H., D. Rudnick, C. Paulson, S. D. Pierce, W. S. Pegau, J. Mickett and M. C. Gregg, 2005: Upper ocean heat and freshwater budgets in the eastern Pacific warm pool. *J. Geophys. Res.*, 110, doi:10.1029/2004JC002511.

Uhlhorn, E. W and L.K. Shay, 2004: Analysis of Upper-Ocean thermodynamic observations forced by Hurricane Lili. 26th Conference on Hurricane and Tropical Meteorology, AMS 3-7 May, Miami Beach, FL, 619-620.